Author/s:
Steiner, A;Rybak, K;Altmann, M;McFarlane, HE;Klaeger, S;Nguyen, N;Facher, E;Ivakov, A;Wanner, G;Kuster, B;Persson, S;Braun, P;Hauser, MT;Assaad, FF

Title:
Cell cycle-regulated PLEIADE/AtMAP65-3 links membrane and microtubule dynamics during plant cytokinesis

Date:
2016-11-01

Citation:
Steiner, A., Rybak, K., Altmann, M., McFarlane, H. E., Klaeger, S., Nguyen, N., Facher, E., Ivakov, A., Wanner, G., Kuster, B., Persson, S., Braun, P., Hauser, M. T. & Assaad, F. F. (2016). Cell cycle-regulated PLEIADE/AtMAP65-3 links membrane and microtubule dynamics during plant cytokinesis. Plant Journal, 88 (4), pp.531-541. https://doi.org/10.1111/tpj.13275.

Received Date : 02-Mar-2015
Accepted Date : 27-Jun-2016
Article type : Original Article

Cell cycle-regulated PLEIADE/AtMAP65-3 links membrane and microtubule dynamics during plant cytokinesis

Alexander Steiner[1], Katarzyna Rybak[1], Melina Altmann[2], Heather E. McFarlane[3,7], Susan Klaeger[4], Ngoc Nguyen[1], Eva Facher[5], Alexander Ivakov[3,7], Gerhard Wanner[5], Bernhard Kuster[4], Staffan Persson[3,6,7], Pascal Falter-Braun[2], Marie-Theres Hauser[8] and Farhah F. Assaad[1*]

[1] Botany, Technische Universität München, 85354 Freising, Germany
[2] Plant Systems Biology, Technische Universität München, 85354 Freising, Germany
[3] School of Biosciences, University of Melbourne, Parkville 3010, Victoria, Australia
[4] Chair of Proteomics and Bioanalytics, Technische Universität München, 85354 Freising, Germany
[5] Department Biologie I, Ludwig-Maximillians Universität, 82152 Planegg-Martinsried, Germany
[6] ARC Centre of Excellence in Plant Cell Walls, School of Biosciences, University of Melbourne, Parkville 3010, Victoria, Australia
[7] Max Planck Institute for Molecular Plant Physiology, 14476 Postdam, Germany
[8] Department of Applied Genetics and Cell Biology, University of Natural Resources and Life Sciences, 1190 Vienna, Austria

* corresponding author
Botany Department
Technische Universität München
Emil-Ramann-Str. 4
85354 Freising

Germany
Farhah@wzw.tum.de
Tel: +49-8161-71-5437
FAX: +49-8161-71-5432

Email addresses of all coauthors
Alexander Steiner <steinera@wzw.tum.de>
katarzyna.rybak <katarzyna.rybak@o2.pl>
Melina Altmann <melina.altmann@wzw.tum.de>
Kläger, Susan <susan.klaeger@tum.de>
Heather McFarlane <heather.mcfarlane@unimelb.edu.au>
Ngoc Nguyen <n.t.k.nguyen@qmul.ac.uk>
Eva Facher <e.facher@lrz.uni-muenchen.de>
Alexander Ivakov <Alexandre.Ivakov@unimelb.edu.au>
Gerhard Wanner <Wanner@lrz.uni-muenchen.de>
Bernhard Kuster <kuster@tum.de>
Staffan Persson <Staffan.persson@unimelb.edu.au>
Pascal Falter-Braun <pbraun@wzw.tum.de>
Marie-Theres Hauser <marie-theres.hauser@boku.ac.at>
Farhah Assaad <farhah@wzw.tum.de>

Running title:
A TRAPPII-MAP65 interaction module

Key Words:
Cytokinesis, phragmoplast microtubules, cell plate, MAP65-3/PLEAIDE, TRAPPII, CLUB/TRS130, AtTRS120, Arabidopsis thaliana.

SUMMARY
Cytokinesis, the partitioning of the cytoplasm following nuclear division, requires extensive coordination between cell cycle cues, membrane trafficking and microtubule dynamics. Plant cytokinesis occurs within a transient membrane compartment known as the cell plate, to which vesicles are delivered by a plant-specific microtubule array, the phragmoplast. While membrane proteins required for cytokinesis are known, how these are coordinated with microtubule dynamics and regulated by cell cycle cues remains unclear. Here, we document physical and genetic interactions between

Transport Protein Particle II (TRAPPII) tethering factors and microtubule-associated proteins of the PLEIADE/AtMAP65 family. These interactions do not specifically affect the recruitment of either TRAPPII or MAP65 proteins to the cell plate or midzone. Rather, and based on single versus double mutant phenotypes, it appears that they are required to coordinate cytokinesis with the nuclear division cycle. As MAP65 family members are known to be targets of cell cycle regulated kinases, our results provide a conceptual framework for how membrane and microtubule dynamics may be coordinated with each other and with the nuclear cycle during plant cytokinesis.

INTRODUCTION

In plants, the onset of cytokinesis is characterized by the assembly of a plant-specific microtubule array, the phragmoplast. Phragmoplast microtubules are initially organized in a solid array. As cells enter telophase, microtubules are translocated to the leading edges of the phragmoplast, giving rise to a ring-shaped phragmoplast (Müller and Jürgens, 2015). Recent studies have addressed the transition from the solid to the ring-shaped phragmoplast (for review see Lee and Liu, 2013). The centrifugal expansion that underlies this transition is a result of continuous microtubule assembly at the periphery of the phragmoplast concomitant with the disassembly of microtubules towards the center of the phragmoplast (Smertenko et al., 2011). New microtubules are nucleated on existing phragmoplast microtubules (Murata et al., 2013). Nucleation requires γ-tubulin, which is an essential and conserved component of plant and animal MTOCs. γ-tubulin is found at the phragmoplast, with a preference for microtubule minus ends at the distal edges facing the daughter nuclei; it is not found at the phragmoplast midzone (Kong et al., 2010). At the plus end, bundling of antiparallel microtubules coming from opposite sides of the division plane occurs selectively at the periphery of the phragmoplast. Bundling is mediated by the dimerization of microtubule cross-linking proteins of the MAP65 family, notably the cytokinesis-specific MAP65-3/PLEIADE member (Müller et al., 2002, 2004; Ho et al., 2012; Murata et al., 2013). The Arabidopsis MAP65 family encodes plant-specifc microtubule-associated proteins (MAPs) that have been shown to bind and bundle microtubules *in vitro* (Chan et al., 2003; Van Damme et al., 2004; Gaillard et al., 2008). The debundling of microtubules towards the center of the phragmoplast is mediated via phosphorylation of MAP65-3/PLEIADE by mitogen-activated protein MAP kinases (Takahashi et al., 2004). The MAP kinase cascade is, in turn, activated in a cell cycle dependent fashion by the Kinesin 7 member NACK1/HINKEL (Sasabe et al., 2006, 2011a; Vanstraelen et al., 2006). The NACK1/NACK2 kinesin-like proteins, together with the MAPK cascade, comprise the NACK-PQR pathway

(Lee and Liu, 2013). Debundled microtubules are thought to be severed and disassembled via the action of katanin (Panteris et al., 2011).

The organization of the phragmoplast microtubule array requires KINESIN 12A/12B motors, which specifically decorate the plus end of phragmoplast microtubules in a MAP65-3 dependent manner (Lee et al., 2007; Ho et al., 2011). Phragmoplast microtubules are organized in an antiparallel array with their plus ends facing the division plane, such that transport from both sides of a dividing cell delivers vesicles to the cell equator. At the equator, the nascent cross wall is assembled within the lumen of a transient membrane compartment referred to as the cell plate. The execution of plant cytokinesis requires a number of trafficking components involved in vesicle formation, tethering, docking and fusion (Ebine and Ueda, 2015; Müller and Jürgens, 2015). The BIG ARF-GEFs have recently been shown to regulate cytokinetic vesicle formation (Richter et al., 2014). The Transport Protein Particle II (TRAPPII) tethering complex and interacting Rab-GTPases are required for cell plate formation (Chow et al., 2008; Jaber et al., 2010; Qi and Zheng, 2011; Qi et al., 2011; Rybak et al., 2014; for review see Kim et al., 2016). Later in cytokinesis, the exocyst tethering complex is involved cell plate maturation (Fendrych et al., 2010; Rybak et al., 2014; reviewed by Boruc and Van Damme, 2015). Membrane fusion events at the cell plate are predominantly mediated by the t-SNARE KNOLLE and its interacting partner, the SM/Sec1 protein KEULE (Waizenegger et al., 2000; Assaad et al., 2001; Park et al., 2012; for review see Müller and Jürgens, 2015) . While membrane proteins required for cytokinesis are known, how these are coordinated with microtubule dynamics and regulated by cell cycle cues remains to be elucidated.

In this study, we document physical and genetic interactions between membrane and microtubule components of cytokinesis. We first identified membrane related cytokinesis components whose localization dynamics best follow phragmoplast microtubule array organization. We then used these membrane-related proteins as baits for immunoprecipitation experiments. Copurified proteins, identified by mass spectrometry, were mined for proteins interacting with microtubule plus ends. We subsequently focused on the most interesting pair of membrane related proteins and MAPs: the TRAPPII - MAP65 interaction. The mass spectrometry data were validated with binary interaction assays, double mutant analyses and an analysis of co-localization. An appraisal of single versus double mutant phenotypes lead us to outline a conceptual framework for the coordination between membrane and cytoskeletal dynamics and their regulation by cell cycle cues during plant cytokinesis.

RESULTS and DISCUSSION

The TRAPPII tethering complex interacts with MAP65 family members

To identify interactions that govern the coordination between membrane and microtubule dynamics during cytokinesis, we performed immunoprecipitation experiments with mass spectrometry readout. We first monitored seven membrane-related markers (Table S1) for their localization dynamics at the cell plate, in conjunction with a microtubule marker (Gutierrez et al., 2009). Of these, the Sec1/Munc18 protein KEULE-GFP (Steiner et al., 2016) as well as the TRAPPII tethering factors TRS120-GFP and CLUB/AtTRS130-GFP (Rybak et al., 2014) best followed microtubule array reorganization from the solid to the ring-shaped phragmoplast stages. These three markers were subsequently used as baits and the mass spectrometry data were mined for potential microtubule-related hits.

An abundance of tubulin subunits and several proteins associated with microtubule plus-end tracking (+TIP; Bisgrove et al., 2004; Hamada, 2014) were enriched in TRAPPII but not in KEULE pulldowns (Table I; Table S2). Interestingly, six unique peptides corresponding to Arabidopsis Microtubule Associated Protein 65 (MAP65) proteins (Smertenko et al., 2004; Van Damme et al., 2004; Sasabe et al., 2011b; Ho et al., 2012)) co-purified with CLUB-GFP and five with AtTRS120-GFP; of these, four peptides were identified in both TRAPPII pull downs (Table I; Table S2; Figure S1). The signals showed strong intensity, a significant enrichment over the control (empty GFP-cassette) and a significant P value of 0.008 across three biological replicates. Considering that genes that are co-expressed tend to be involved in related biological processes (Usadel et al., 2009), we evaluated co-expression coefficients using Genevestigator (Hruz et al., 2008; Table I). This identified positive correlations in a number of cases, with numbers in the 0.5 range that are similar to those found for known TRAPP components (see Table S2), which supports our proteomic data.

We focused on microtubule-associated proteins of the MAP65 family, which are known to bundle and stabilize the plus end of microtubules *in vitro* (Smertenko et al., 2004; Gaillard et al., 2008). The Arabidopsis MAP65 family consists of nine members of which three, AtMAP65-1, AtMAP65-2 and PLEIADE (also known as AtMAP65-3), have been shown to act redundantly during cytokinesis (Sasabe et al., 2011b). To test for binary interactions, we performed yeast two hybrid (Y2H) and bifluorescence complementation (BiFC) assays. The full-length CLUB/AtTRS130 and AtTRS120 TRAPPII proteins were poorly expressed in yeast and, in our hands, did not work for Y2H. We, therefore, constructed truncations. CLUB/AtTRS130 and AtTRS120 have conserved TRAPPII domain structures that span the entire length of the protein (Koumandou et al., 2007). Truncations were designed via phylogenetic analysis and the proteins accordingly split into highly conserved (C1, T1), intermediate or mixed (C2, T2) and plant-specific (C3, T3) moieties (Figure 1a). In yeast, the CLUB C3 plant-specific fragment yielded strong interactions with PLEIADE/AtMAP65-3 but the C1 and C2 fragments did not (Figure 1b). Bifluorescence complementation (BiFC) confirmed interactions between TRAPPII subunits and both AtMAP65-1 and PLEIADE/AtMAP65-3

(Figure 1c). While TRAPPII interactions were localized to membranes or to the cytosol, the TRAPPII – MAP65 interactions localized to an ordered, linear array that resembled cortical microtubules (Figure 1c).

For an assessment of genetic interaction, we focused on PLEIADE/AtMAP65-3 because it has a specific cytokinesis-defective phenotype reminiscent of *keule* and of TRAPPII mutants (Smertenko et al., 2004). Indeed, *pleiade* null mutants were identified in the same screens as *club* (Söllner et al., 2002) and *keule* (Gillmor et al., 2016). Double mutant analysis showed synergistic genetic interactions for *ple-2 trs120*-4 double mutants, in which we combined a hypomorphic, viable *ple-2* allele with a null seedling lethal allele of the TRAPPII-specific subunit TRS120 (Figure 2). An additional line of evidence for an interaction is the observation that the TRAPPII subunit TRS120-mCherry (Rybak et al., 2014), which co-localizes with CLUB-GFP at the cell plate (Figure S2), co-localizes with GFP-PLEIADE (Steiner et al., 2016) throughout cytokinesis (Figure 3; Figure S2).

The TRAPPII complex does not appear to act as a membrane anchor for GFP-PLEIADE at the cell plate

To assess the biological relevance of the interactions between PLEIADE/AtMAP65-3 and TRAPPII in the specific context of plant cytokinesis, we first tested whether the TRAPPII membrane tether acts as an anchor for PLEIADE/AtMAP65-3 at the phragmoplast midzone by monitoring GFP-PLEIADE in *TRAPPII* mutants. GFP-PLEIADE was localized at the phragmoplast midzone in both wild-type and *TRAPPII* mutants, but the signal was sometimes discontinuous in *club-2* (Figure 4a). In *club-2* the phragmoplast microtubules were at times also discontinuous in their appearance (Figure 4b), reminiscent of patchy cell plates seen in this mutant line (Rybak et al., 2014). With antibody stains we observed 14% patchy phragmoplasts in *club-2* mutants, as compared to 0.4 % in the wild type (n = 83 *club-2* or 228 wild-type telophase cells), and there was a 100 % correlation between patchy cell plates and patchy phragmoplasts (n = 12) in *club-2*. We conclude that the TRAPPII complex does not appear to act as a membrane anchor for GFP-PLEIADE at the cell plate.

PLEIADE/AtMAP65-3 is not essential for recruiting the TRAPPII complex to the cell plate

We next tested whether, conversely, PLEIADE/AtMAP65-3 may be required for the delivery of the TRAPPII complex to the cell plate. To this effect, we imaged TRS120-GFP in the *ple-4* mutant background. In 78% of cases, (n = 18), we found that the cell plate localization of TRS120-GFP was considerably more diffuse in the *ple-4* mutant background than in the wild-type (Figure 4c and 4d). PLEIADE/AtMAP65-3 is known to bundle antiparallel microtubules coming from opposite sides of the division plane, and as a consequence

pleiade mutants are characterized by a larger midzone gap (Müller et al., 2004; Ho et al., 2012). The observed defect in TRS120-GFP localization in the *ple-4* background was also seen with the FM4-64 stain (Figure 4c and 4d) and may reflect the larger midzone characteristic of *pleiade* mutants rather than a specific defect resulting from a direct interaction between PLEIADE/AtMAP65-3 and the TRAPPII complex. Indeed, the increased cell plate thickness we observe (1.2 µm; Figure 4d) corresponds to the enlarged width of the midzone gap reported in *pleiade* null alleles (1.2 µm; Ho et al., 2012). Overall, in both the wild-type and *ple-4* mutant backgrounds, TRS120-GFP was recruited to the cell plate, reorganized to the leading edges as the cell plate expanded, and was removed from the cell plate at the end of cytokinesis (compare Figure 4c to Figure S2). These results imply that PLEIADE/AtMAP65-3 is not essential for recruiting the TRAPPII complex to the developing cell plate.

The nuclear cycle and cytokinesis appeared to be uncoupled in *pleiade/map65-3 trs120* double mutants

As TRAPPII or PLEIADE/AtMAP65-3 did not appear to specifically affect one another's localization dynamics during cytokinesis, we probed the significance of the interaction by carrying out a more thorough analysis of double mutant phenotypes. Immunofluorescence assays showed that *ple-2 trs120-4* double mutants had a synthetically enhanced number of cells in which four or more nuclei were clumped together in the apparent absence of even vestigial cross walls (Figure 5a-c). Cells with four or more nuclei were never observed in the wild-type or in *trs120-4* single mutants, occurred at a frequency of 0.6% in *ple-2* hypomorphs (n = 4136 cells), and of 12.1% in double mutant cells (n = 1185 cells; Figure 5c). This twenty-fold enhancement between *ple-2* and *ple-2 trs120-4* was highly significant ($p = 3.3\ e^{-05}$) and provided further evidence for a genetic interaction. In summary, in the double mutants the nuclear cycle and cytokinesis appeared to be uncoupled.

The interesting difference between *ple-2* hypomorphs and *trs120-4* null mutants with respect to the incidence of multinucleate cells prompted us to reevaluate the *ple-4* null phenotype. To this effect, we carried out histological sections (Figure 5d) and Focused Ion Beam/Scanning Electron Microscopy (FIB/SEM), which allows for 3D reconstructions at high resolution (Figure 5e). FIB/SEM tomographic datasets occasionally showed binucleate cells in which the cross wall was entirely absent in *ple-4* null mutants (Figure 5e). By contrast, FIB/SEM of *trs120-4* single mutants invariably revealed at least rudimentary cross walls between daughter nuclei (Rybak et al., 2014). Thus, in the double mutant, the *trs120-4* allele synthetically enhances a nuclear phenotype that it itself does not manifest on its own. The contrast between the single mutants further highlights the significance of the synergistic enhancement of the multinucleate phenotype in *ple-2 trs120-4* double mutants (Figure 5a-c).

Progression through the cell cycle involves four key transitions: entry into S-phase, entry into mitosis, exit from mitosis and fourth, the onset and execution of cytokinesis. The key regulators of the first three transitions, which include cyclin-dependent kinases and the anaphase promoting complex, appear to be conserved across kingdoms (Assaad, 2001). The last stage of the cell cycle, however, appears to be different in plants as compared to both fungi and animals. Indeed, in plants a mitogen-activated protein (MAP) kinase cascade, rather than polo kinases, have been shown to regulate plant cytokinesis (Sasabe et al., 2006; Kosetsu et al., 2010). The MAP kinase cascade is activated in a cell cycle dependent fashion and, in turn, targets MAP65 proteins (Sasabe et al., 2006, 2011a; Kosetsu et al., 2010; Müller and Jürgens, 2015). It is interesting that the plant-specific moiety of CLUB/AtTRS130 interacts with PLEIADE/AtMAP65-3. This highlights the unique features of plant cytokinesis, which include the phragmoplast microtubule array and the nature of its cell cycle regulation.

The TRAPPII complex is required for cell plate biogenesis throughout cytokinesis, from cell plate initiation to insertion (Rybak et al., 2014), and it is possibly at this level that cell cycle regulation would be most effective. If the biological role of the TRAPPII-MAP65 interaction were to transmit cell cycle cues to cell plate membranes, we would predict that TRAPPII mutants should have additional phenotypes related to those of targeted MAP65 mutants insensitive to cell-cycle cues. In tobacco, such mutants are severely impaired in centrifugal phragmoplast expansion from the solid to the ring shaped phragmoplast stages (Sasabe et al., 2006). Phragmoplast expansion is also blocked in Arabidopsis Fused kinase TWO-IN-ONE (TIO) mutants; the TIO kinase interacts both with KINESIN 12 and with the NACK-PQR pathway that targets PLEAIDE/AtMAP65-3 (Oh et al., 2005, 2012, 2014). Thus, the NACK-PQR-MAP65 signal transduction pathway appears to act as a major node to regulate phragmoplast expansion. This consideration led us to monitor phragmoplast microtubule reorganization in TRAPPII *club-2* and *trs120-4* mutants. Both live cell imaging (Movies S1-S3; Figure S3) and antibody stains showed a pronounced defect in phragmoplast microtubule reorganization from the solid to the ring-shaped stages in both *club-2* and *trs120-4* (Figure S3). The live imaging shows that there is a delay but not an absolute block in the transition (Movies S1-S3). This is entirely consistent with our hypothesis.

CONCLUSION and PERSPECTIVE

On the basis of the molecular functions of the interacting partners and of single versus double mutant phenotypes, we outline a conceptual framework (Figure 5f) for the integration of membrane dynamics, phragmoplast microtubule dynamics and the nuclear division cycle throughout cytokinesis. PLEIADE/AtMAP65-3 has recently been shown to interact with spindle assembly checkpoint (SAC) proteins in Arabidopsis (Paganelli et al.,

2015). The SAC ensures error-free chromosome segregation by preventing the onset of anaphase as long as any unattached or incorrectly attached chromosomes are present. Thus, PLEIADE/AtMAP65-3 ultimately transmits cues pertaining not only to cell cycle progression but also to chromosome attachment to phragmoplast microtubules. The confirmed TRAPPII-MAP65 interaction would enable these cues to be coordinated with membrane dynamics during cytokinesis. To avoid bisecting the nucleus, it is critical that cross wall deposition be coordinated with cell cycle cues. Our findings provide a conceptual framework for how this might be achieved. Knowledge of checkpoints acting after the spindle assembly checkpoint is lacking (Musacchio, 2015), yet the striking phenotype of the *pleiade trs120* double mutants, in which the nuclear cycle and cytokinesis appear to be uncoupled, tempts one to speculate as to the existence of a cytokinesis checkpoint. The unusual distribution of an Arabidopsis SAC protein at the phragmoplast midzone during cytokinesis has formerly led to similar speculation (Caillaud et al., 2009). The TRAPPII – MAP65 interaction might, in fact, comprise a safeguard mechanism that coordinates the completion of cytokinesis with cell cycle progression beyond anaphase.

EXPERIMENTAL PROCEDURES

Lines and growth conditions

Seedling lethal mutant lines (Table S3) were propagated as hetero- or hemi-zygotes. Plants were grown in the greenhouse under controlled temperature conditions and with supplemental light, or under controlled growth chamber conditions (16/8 hr photoperiod at 250 µmol $m^{-2}s^{-1}$). Seed were surface sterilized, stratified at 4˚C for two days and plated on MS medium supplemented with 1% sucrose and B5 Vitamins (Sigma). The root tips or hypocotyls of five-day old plate grown seedlings were used for imaging.

Molecular methods

TRAPPII truncations were constructed via Gateway cloning as described in the Supporting Information Methods S1, using full length cDNA clones obtained from the RIKEN Bioresource Center (Seki et al., 2002).

Co-immunoprecipitation

Co-immunoprecipitation experiments were carried out on three grams of leaves, seedlings or inflorescences using GFP-trap beads (Chromotek) or anti-HA beads (Roche), as described (Park et al., 2012 with modifications described in Rybak et al., 2014). NanoflowLc-MS/MS was performed by coupling an EksigentnanoLC-Ultra 1D+ (Eksigent, Dublin, CA) to a Velos-

LTQ-Orbitrap (Thermo Scientific, Bremen, Germany; see Supporting Information Methods S2).

Yeast two hybrid (Y2H)

Y2H screens were performed as described (Dreze et al., 2010). Briefly, open reading frames (ORFs) encoding fragments of CLUB/AtTRS130 (C1-C3) and TRS120 (T1, T2, T3) were transferred by Gateway cloning into the GAL4 DNA-binding domain (DB) encoding Y2H vector pDEST-pPC97, and subsequently transformed into the yeast strain Y8930. These constructs were screened by yeast mating against a collection of 12,000 Arabidopsis ORFs fused to the Gal4 activation domain (AD) in the yeast strain Y8800 (Weßling et al., 2014). Screening was done as a binary mini-pool screen, *i.e.* each DB-ORF was screened against pools of 188 AD-ORFs. Interactions were assayed by growth on selective plates using the *HIS3* reporter, and using 1mM 3-Amino-1,2,4-triazole (3-AT) to suppress background growth. This primary screen was carried out once and interaction candidates were identified by Sanger sequencing. All candidate interactions were verified by pairwise one-on-one mating in three independent experiments. Only pairs scoring positives in all three assays were considered as *bona fide* interaction partners.

Bifluorescence complementation

Agrobacterium carrying individual vectors were co-infiltrated into young *Nicotiana benthamiana* leaves in a solution of 10mM MES, 10mM $MgCl_2$, and 100µm acetosyringone with each Agrobacterium vector strain (Gookin and Assmann, 2014) at OD_{600}=0.03. Combinations are indicated in figure panels. BiFC signal was visualized using a Leica SP2 confocal microscope with 514nm excitation and 525-600nm emission filter to detect YFP. See Supporting Information Methods S3.

Antibody stains and confocal microscopy. Root tips were fixed in paraformaldehyde, permeablized and stained according to (Völker et al., 2001), with anti-KNOLLE (Lauber et al., 1997) (rabbit, 1:2000), anti-tubulin (mouse, 1:2500, Sigma), anti-rabbit monoclonal Alexa-m488 (goat, 1:600, Molecular Probes) as well as anti-mouse Cy3 (goat, 1:600, Dianova). Nuclei were stained with 1µg/ml DAPI (Sigma). A Fluoview 1000 confocal laser scanning microscope (Olympus) was used for images acquisition and processing.

Light and Electron microscopy

Histological embryo sections were prepared and imaged as described (Assaad et al., 1996). Fresh seedlings were imaged in low vacuum with a Zeiss (LEO) VP 438 scanning electron microscope operated at 15 kV. For electron microscopy, root tips were fixed by high-pressure

freezing and freeze substituted (Leica HPM100; Leica ASF2) and FIB/SEM tomographic datasets were acquired with a Zeiss-Auriga workstation (Carl Zeiss Microscopy) as described in the Supporting Information Methods S4.

Statistical and Image analyses

False discovery rates, determined with the standard two-tailed t-test, were set at a cutoff of 1%. Images were processed with Adobe photoshop, analyzed with Image J, and assembled with Adobe Illustrator. 3D reconstructions were carried out with Imaris software (Bitplane).

Acknowledgement

We thank Prof. Grill and members of the Botany department for their support. Silvia Dobler in the laboratory of Andreas Klingl (LMU) prepared samples for electron microscopy. Rosi Söllner performed histological sections. David Ehrhardt, Gerd Jürgens and the RIKEN Bioresource Center shared published or public resources. HEM is supported by an EMBO Long-Term Fellowship (EMBO ALTF 1246-2013) and an NSERC PDF (PDF-454454-2014); AI and SP were funded by the Max-Planck-Gesellschaft, and SP by a R@MAP Professorship at University of Melbourne. This research was funded by DFG grant AS110/5-1 to FFA and GW and by the FWF grant P16410-B12 to MTH. The authors declare no conflict of interest.

SUPPORTING INFORMATION

Figure S1. AtMAP65-1 peptides identified in TRAPPII immunoprecipitated complexes. Related to Figure1.

Figure S2. TRS120-mCherry co-localizes with CLUB-GFP at the cell plate. Related to Figure 3.

Figure S3. Impairment of microtubule reorganization in *club-2* and *trs120-4* mutants. Related to Figure 5.

Table S1. Marker lines used in this analysis.

Table S2. Analysis of CLUB-GFP immunoprecipitates via mass spectrometry.

Table S3. Mutant lines used in this study.

Movie S1. Microtubule reorganization in the wild-type. Related to Figures 5 and S3.

Movie S2. Delayed microtubule reorganization in *club-2*. Related to Figures 5 and S3.

Movie S3. Delayed microtubule reorganization in *trs120-4*. Related to Figures 5 and S3.

Methods.

REFERENCES

Ambrose, J.C., and Wasteneys, G.O. (2008). CLASP Modulates Microtubule-Cortex Interaction during Self-Organization of Acentrosomal Microtubules. Mol. Biol. Cell *19*, 4730–4737.

Ambrose, C., Allard, J.F., Cytrynbaum, E.N., and Wasteneys, G.O. (2011). A CLASP-modulated cell edge barrier mechanism drives cell-wide cortical microtubule organization in Arabidopsis. Nat. Commun. *2*, 430.

Ambrose, J.C., Shoji, T., Kotzer, A.M., Pighin, J.A., and Wasteneys, G.O. (2007). The Arabidopsis CLASP Gene Encodes a Microtubule-Associated Protein Involved in Cell Expansion and Division. Plant Cell *19*, 2763–2775.

Assaad, F.F. (2001). Of weeds and men: what genomes teach us about plant cell biology. Curr. Opin. Plant Biol. *4*, 478–487.

Assaad, F.F., Mayer, U., Wanner, G., and Jürgens, G. (1996). The KEULE gene is involved in cytokinesis in Arabidopsis. Mol. Gen. Genet. MGG *253*, 267–277.

Assaad, F.F., Huet, Y., Mayer, U., and Jürgens, G. (2001). The Cytokinesis Gene KEULE Encodes a Sec1 Protein That Binds the Syntaxin Knolle. J. Cell Biol. *152*, 531–544.

Boruc, J., and Van Damme, D. (2015). Endomembrane trafficking overarching cell plate formation. Curr. Opin. Plant Biol. *28*, 92–98.

Caillaud, M.-C., Paganelli, L., Lecomte, P., Deslandes, L., Quentin, M., Pecrix, Y., Le Bris, M., Marfaing, N., Abad, P., and Favery, B. (2009). Spindle Assembly Checkpoint Protein Dynamics Reveal Conserved and Unsuspected Roles in Plant Cell Division. PLoS ONE *4*.

Chan, J., Mao, G., Smertenko, A., Hussey, P.J., Naldrett, M., Bottrill, A., and Lloyd, C.W. (2003). Identification of a MAP65 isoform involved in directional expansion of plant cells. FEBS Lett. *534*, 161–163.

Chow, C.-M., Neto, H., Foucart, C., and Moore, I. (2008). Rab-A2 and Rab-A3 GTPases Define a trans-Golgi Endosomal Membrane Domain in Arabidopsis That Contributes Substantially to the Cell Plate. Plant Cell *20*, 101–123.

Dreze, M., Monachello, D., Lurin, C., Cusick, M.E., Hill, D.E., Vidal, M., and Braun, P. (2010). Chapter 12 - High-Quality Binary Interactome Mapping. B.-M. in Enzymology, ed. (Academic Press), pp. 281–315.

Ebine, K., and Ueda, T. (2015). Roles of membrane trafficking in plant cell wall dynamics. Front. Plant Sci. *6*, 878.

Eleftheriou, E.P., Baskin, T.I., and Hepler, P.K. (2005). Aberrant cell plate formation in the Arabidopsis thaliana microtubule organization 1 mutant. Plant Cell Physiol. *46*, 671–675.

Fendrych, M., Synek, L., Pečenková, T., Toupalová, H., Cole, R., Drdová, E., Nebesářová, J., Šedinová, M., Hála, M., Fowler, J.E., et al. (2010). The Arabidopsis Exocyst Complex Is Involved in Cytokinesis and Cell Plate Maturation. Plant Cell *22*, 3053–3065.

Gaillard, J., Neumann, E., Van Damme, D., Stoppin-Mellet, V., Ebel, C., Barbier, E., Geelen, D., and Vantard, M. (2008). Two Microtubule-associated Proteins of Arabidopsis MAP65s Promote Antiparallel Microtubule Bundling. Mol. Biol. Cell *19*, 4534–4544.

Gillmor, C.S., Roeder, A.H.K., Sieber, P., Somerville, C., and Lukowitz, W. (2016). A Genetic Screen for Mutations Affecting Cell Division in the Arabidopsis thaliana Embryo Identifies Seven Loci Required for Cytokinesis. PLOS ONE *11*, e0146492.

Gookin, T.E., and Assmann, S.M. (2014). Significant reduction of BiFC non-specific assembly facilitates in planta assessment of heterotrimeric G-protein interactors. Plant J. *80*, 553–567.

Gutierrez, R., Lindeboom, J.J., Paredez, A.R., Emons, A.M.C., and Ehrhardt, D.W. (2009). Arabidopsis cortical microtubules position cellulose synthase delivery to the plasma membrane and interact with cellulose synthase trafficking compartments. Nat. Cell Biol. *11*, 797–806.

Ho, C.-M.K., Hotta, T., Guo, F., Roberson, R.W., Lee, Y.-R.J., and Liu, B. (2011). Interaction of Antiparallel Microtubules in the Phragmoplast Is Mediated by the Microtubule-Associated Protein MAP65-3 in Arabidopsis. Plant Cell *23*, 2909–2923.

Ho, C.-M.K., Lee, Y.-R.J., Kiyama, L.D., Dinesh-Kumar, S.P., and Liu, B. (2012). Arabidopsis Microtubule-Associated Protein MAP65-3 Cross-Links Antiparallel Microtubules toward Their Plus Ends in the Phragmoplast via Its Distinct C-Terminal Microtubule Binding Domain[W]. Plant Cell *24*, 2071–2085.

Hruz, T., Laule, O., Szabo, G., Wessendorp, F., Bleuler, S., Oertle, L., Widmayer, P., Gruissem, W., and Zimmermann, P. (2008). Genevestigator V3: A Reference Expression Database for the Meta-Analysis of Transcriptomes. Adv. Bioinforma. *2008*, e420747.

Jaber, E., Thiele, K., Kindzierski, V., Loderer, C., Rybak, K., Jürgens, G., Mayer, U., Söllner, R., Wanner, G., and Assaad, F.F. (2010). A putative TRAPPII tethering factor is required for cell plate assembly during cytokinesis in Arabidopsis. New Phytol. *187*, 751–763.

Kawamura, E., Himmelspach, R., Rashbrooke, M.C., Whittington, A.T., Gale, K.R., Collings, D.A., and Wasteneys, G.O. (2006). MICROTUBULE ORGANIZATION 1 regulates structure and function of microtubule arrays during mitosis and cytokinesis in the Arabidopsis root. Plant Physiol. *140*, 102–114.

Kim, J.J., Lipatova, Z., and Segev, N. (2016). TRAPP Complexes in Secretion and Autophagy. Front. Cell Dev. Biol. *4*, 20.

Kirik, V., Herrmann, U., Parupalli, C., Sedbrook, J.C., Ehrhardt, D.W., and Hülskamp, M. (2007). CLASP localizes in two discrete patterns on cortical microtubules and is required for cell morphogenesis and cell division in Arabidopsis. J. Cell Sci. *120*, 4416–4425.

Kong, Z., Hotta, T., Lee, Y.-R.J., Horio, T., and Liu, B. (2010). The {gamma}-tubulin complex protein GCP4 is required for organizing functional microtubule arrays in Arabidopsis thaliana. Plant Cell *22*, 191–204.

Kosetsu, K., Matsunaga, S., Nakagami, H., Colcombet, J., Sasabe, M., Soyano, T., Takahashi, Y., Hirt, H., and Machida, Y. (2010). The MAP kinase MPK4 is required for cytokinesis in Arabidopsis thaliana. Plant Cell *22*, 3778–3790.

Koumandou, V.L., Dacks, J.B., Coulson, R.M., and Field, M.C. (2007). Control systems for membrane fusion in the ancestral eukaryote; evolution of tethering complexes and SM proteins. BMC Evol. Biol. *7*, 29.

Lauber, M.H., Waizenegger, I., Steinmann, T., Schwarz, H., Mayer, U., Hwang, I., Lukowitz, W., and Jürgens, G. (1997). The Arabidopsis KNOLLE Protein Is a Cytokinesis-specific Syntaxin. J. Cell Biol. *139*, 1485–1493.

Lechner, B., Rashbrooke, M.C., Collings, D.A., Eng, R.C., Kawamura, E., Whittington, A.T., and Wasteneys, G.O. (2012). The N-terminal TOG domain of Arabidopsis MOR1 modulates affinity for microtubule polymers. J. Cell Sci. *125*, 4812–4821.

Lee, Y.-R.J., and Liu, B. (2013). The rise and fall of the phragmoplast microtubule array. Curr. Opin. Plant Biol. *16*, 757–763.

Lee, Y.-R.J., Li, Y., and Liu, B. (2007). Two Arabidopsis phragmoplast-associated kinesins play a critical role in cytokinesis during male gametogenesis. Plant Cell *19*, 2595–2605.

Mao, G., Chan, J., Calder, G., Doonan, J.H., and Lloyd, C.W. (2005). Modulated targeting of GFP-AtMAP65-1 to central spindle microtubules during division. Plant J. Cell Mol. Biol. *43*, 469–478.

Müller, S., and Jürgens, G. (2015). Plant cytokinesis-No ring, no constriction but centrifugal construction of the partitioning membrane. Semin. Cell Dev. Biol.

Müller, S., Fuchs, E., Ovecka, M., Wysocka-Diller, J., Benfey, P.N., and Hauser, M.-T. (2002). Two New Loci, PLEIADE and HYADE, Implicate Organ-Specific Regulation of Cytokinesis in Arabidopsis. Plant Physiol. *130*, 312–324.

Müller, S., Smertenko, A., Wagner, V., Heinrich, M., Hussey, P.J., and Hauser, M.-T. (2004). The Plant Microtubule-Associated Protein AtMAP65-3/PLE Is Essential for Cytokinetic Phragmoplast Function. Curr. Biol. CB *14*, 412–417.

Murata, T., Sano, T., Sasabe, M., Nonaka, S., Higashiyama, T., Hasezawa, S., Machida, Y., and Hasebe, M. (2013). Mechanism of microtubule array expansion in the cytokinetic phragmoplast. Nat. Commun. *4*.

Musacchio, A. (2015). The Molecular Biology of Spindle Assembly Checkpoint Signaling Dynamics. Curr. Biol. *25*, 3017.

Oh, S.A., Johnson, A., Smertenko, A., Rahman, D., Park, S.K., Hussey, P.J., and Twell, D. (2005). A divergent cellular role for the FUSED kinase family in the plant-specific cytokinetic phragmoplast. Curr. Biol. CB *15*, 2107–2111.

Oh, S.A., Allen, T., Kim, G.J., Sidorova, A., Borg, M., Park, S.K., and Twell, D. (2012). Arabidopsis Fused kinase and the Kinesin-12 subfamily constitute a signalling module required for phragmoplast expansion. Plant J. Cell Mol. Biol. *72*, 308–319.

Oh, S.A., Bourdon, V., Dickinson, H.G., Twell, D., and Park, S.K. (2014). Arabidopsis Fused kinase TWO-IN-ONE dominantly inhibits male meiotic cytokinesis. Plant Reprod. *27*, 7–17.

Paganelli, L., Caillaud, M.-C., Quentin, M., Damiani, I., Govetto, B., Lecomte, P., Karpov, P.A., Abad, P., Chabouté, M.-E., and Favery, B. (2015). Three BUB1 and BUBR1/MAD3-related spindle assembly checkpoint proteins are required for accurate mitosis in Arabidopsis. New Phytol. *205*, 202–215.

Panteris, E., Adamakis, I.-D.S., Voulgari, G., and Papadopoulou, G. (2011). A role for katanin in plant cell division: microtubule organization in dividing root cells of fra2 and lue1Arabidopsis thaliana mutants. Cytoskelet. Hoboken NJ *68*, 401–413.

Park, M., Touihri, S., Müller, I., Mayer, U., and Jürgens, G. (2012). Sec1/Munc18 protein stabilizes fusion-competent syntaxin for membrane fusion in Arabidopsis cytokinesis. Dev. Cell *22*, 989–1000.

Pietra, S., Gustavsson, A., Kiefer, C., Kalmbach, L., Hörstedt, P., Ikeda, Y., Stepanova, A.N., Alonso, J.M., and Grebe, M. (2013). Arabidopsis SABRE and CLASP interact to stabilize cell division plane orientation and planar polarity. Nat. Commun. *4*, 2779.

Qi, X., and Zheng, H. (2011). Arabidopsis TRAPPII is functionally linked to Rab-A, but not Rab-D in polar protein trafficking in trans-Golgi network. Plant Signal. Behav. *6*, 1679–1683.

Qi, X., Kaneda, M., Chen, J., Geitmann, A., and Zheng, H. (2011). A specific role for Arabidopsis TRAPPII in post-Golgi trafficking that is crucial for cytokinesis and cell polarity. Plant J. Cell Mol. Biol. *68*, 234–248.

Richter, S., Kientz, M., Brumm, S., Nielsen, M.E., Park, M., Gavidia, R., Krause, C., Voss, U., Beckmann, H., Mayer, U., et al. (2014). Delivery of endocytosed proteins to the cell–division plane requires change of pathway from recycling to secretion. eLife *3*.

Rybak, K., Steiner, A., Synek, L., Klaeger, S., Kulich, I., Facher, E., Wanner, G., Kuster, B., Zarsky, V., Persson, S., et al. (2014). Plant cytokinesis is orchestrated by the sequential action of the TRAPPII and exocyst tethering complexes. Dev. Cell *29*, 607–620.

Sasabe, M., Soyano, T., Takahashi, Y., Sonobe, S., Igarashi, H., Itoh, T.J., Hidaka, M., and Machida, Y. (2006). Phosphorylation of NtMAP65-1 by a MAP kinase down-regulates its activity of microtubule bundling and stimulates progression of cytokinesis of tobacco cells. Genes Dev. *20*, 1004–1014.

Sasabe, M., Boudolf, V., Veylder, L.D., Inzé, D., Genschik, P., and Machida, Y. (2011a). Phosphorylation of a mitotic kinesin-like protein and a MAPKKK by cyclin-dependent kinases (CDKs) is involved in the transition to cytokinesis in plants. Proc. Natl. Acad. Sci. *108*, 17844–17849.

Sasabe, M., Kosetsu, K., Hidaka, M., Murase, A., and Machida, Y. (2011b). Arabidopsis thaliana MAP65-1 and MAP65-2 function redundantly with MAP65-3/PLEIADE in cytokinesis downstream of MPK4. Plant Signal. Behav. *6*, 743–747.

Seki, M., Narusaka, M., Kamiya, A., Ishida, J., Satou, M., Sakurai, T., Nakajima, M., Enju, A., Akiyama, K., Oono, Y., et al. (2002). Functional annotation of a full-length Arabidopsis cDNA collection. Science *296*, 141–145.

Smertenko, A.P., Chang, H.-Y., Wagner, V., Kaloriti, D., Fenyk, S., Sonobe, S., Lloyd, C., Hauser, M.-T., and Hussey, P.J. (2004). The Arabidopsis microtubule-associated protein AtMAP65-1: molecular analysis of its microtubule bundling activity. Plant Cell *16*, 2035–2047.

Smertenko, A.P., Piette, B., and Hussey, P.J. (2011). The origin of phragmoplast asymmetry. Curr. Biol. CB *21*, 1924–1930.

Söllner, R., Glässer, G., Wanner, G., Somerville, C.R., Jürgens, G., and Assaad, F.F. (2002). Cytokinesis-Defective Mutants of Arabidopsis. Plant Physiol. *129*, 678–690.

Steiner, A., Müller, L., Rybak, K., Vodermaier, V., Facher, E., Thellmann, M., Ravikumar, R., Wanner, G., Hauser, M.-T., and Assaad, F.F. (2016). The Membrane-Associated Sec1/Munc18 KEULE is Required for Phragmoplast Microtubule Reorganization During Cytokinesis in Arabidopsis. Mol. Plant *9*, 528–540.

Takahashi, Y., Soyano, T., Sasabe, M., and Machida, Y. (2004). A MAP kinase cascade that controls plant cytokinesis. J. Biochem. (Tokyo) *136*, 127–132.

Twell, D., Park, S.K., Hawkins, T.J., Schubert, D., Schmidt, R., Smertenko, A., and Hussey, P.J. (2002). MOR1/GEM1 has an essential role in the plant-specific cytokinetic phragmoplast. Nat. Cell Biol. *4*, 711–714.

Usadel, B., Obayashi, T., Mutwil, M., Giorgi, F.M., Bassel, G.W., Tanimoto, M., Chow, A., Steinhauser, D., Persson, S., and Provart, N.J. (2009). Co-expression tools for plant biology: opportunities for hypothesis generation and caveats. Plant Cell Environ. *32*, 1633–1651.

Van Damme, D., Van Poucke, K., Boutant, E., Ritzenthaler, C., Inzé, D., and Geelen, D. (2004). In vivo dynamics and differential microtubule-binding activities of MAP65 proteins. Plant Physiol. *136*, 3956–3967.

Vanstraelen, M., Inzé, D., and Geelen, D. (2006). Mitosis-specific kinesins in Arabidopsis. Trends Plant Sci. *11*, 167–175.

Völker, A., Stierhof, Y.D., and Jürgens, G. (2001). Cell cycle-independent expression of the Arabidopsis cytokinesis-specific syntaxin KNOLLE results in mistargeting to the plasma membrane and is not sufficient for cytokinesis. J. Cell Sci. *114*, 3001–3012.

Waizenegger, I., Lukowitz, W., Assaad, F., Schwarz, H., Jürgens, G., and Mayer, U. (2000). The Arabidopsis KNOLLE and KEULE genes interact to promote vesicle fusion during cytokinesis. Curr. Biol. *10*, 1371–1374.

Weßling, R., Epple, P., Altmann, S., He, Y., Yang, L., Henz, S.R., McDonald, N., Wiley, K., Bader, K.C., Glaesser, C., et al. (2014). Convergent Targeting of a Common Host Protein-Network by Pathogen Effectors from Three Kingdoms of Life. CELL HOST MICROBE *16*, 364–375.

Whittington, A.T., Vugrek, O., Wei, K.J., Hasenbein, N.G., Sugimoto, K., Rashbrooke, M.C., and Wasteneys, G.O. (2001). MOR1 is essential for organizing cortical microtubules in plants. Nature *411*, 610–613.

Wightman, R., Chomicki, G., Kumar, M., Carr, P., and Turner, S.R. (2013). SPIRAL2 determines plant microtubule organization by modulating microtubule severing. Curr. Biol. CB *23*, 1902–1907.

Yao, M., Wakamatsu, Y., Itoh, T.J., Shoji, T., and Hashimoto, T. (2008). Arabidopsis SPIRAL2 promotes uninterrupted microtubule growth by suppressing the pause state of microtubule dynamics. J. Cell Sci. *121*, 2372–2381.

Figure Legends

Figure 1. Physical interaction between the TRAPPII complex and MAP65 proteins. See Figure S1.

(a) TRAPPII truncations used for binary interaction assays. Segments colored in red are conserved across kingdoms, while ones in green are plant-specific. The orange moiety of the C2 segment is poorly conserved across kingdoms. The T2 middle segment corresponds to sequences found to interact with the exocyst in a yeast two-hybrid screen (Rybak et al., 2014).

(b) Yeast two-hybrid experiments; the panels are spliced together from different plates. Note positive interactions between the plant specific C3_DB CLUB/AtTRS130 truncation and AtMAP65-3_AD, and between CLUB C2_DB or C3_DB and T2_AD. T2_DB is an auto activator, as evidenced by colony growth with the empty AD vector, and this precludes our ability to determine whether AtTRS120_T2 interacts with PLEIADE/AtMAP65-3.

(c) BiFC experiments. VYNE and VYCE vectors represent fusions of the specified proteins or protein fragments to N- and C-terminal YFP moieties. The CLUB-C3 truncation and

AtTRS120 full-length protein interact with AtMAP65-1 and AtMAP65-3. This interaction is localized to an ordered, linear array reminiscent of cortical microtubules. By contrast, TRAPPII complex interactions (here CLUB_C3 is shown to interact with TRS120) are localized to intracellular membranes and to the cytosol. As a negative control, AtMAP65-1 does not interact with the CLUB_C2 truncation. Bars = 10 µm.

Figure 2. Genetic interaction between the TRAPPII complex and MAP65 proteins.
(a-d) Environmental Scanning Electron Micrographs of wild type and mutant seedlings. Arrows point to cell wall stubs.
Bars = 0.5 mm overview; 20 µm close-up.
(a) wild type.
(b) *ple-2*, a hypomorphic, viable allele of the *AtMAP65-3* locus.
(c) *trs120-4,* a *TRAPPII* null mutant.
(d) *ple-2 trs120-4* double mutant.
(e) % hypocotyl cells with incomplete cross walls in single and double mutants. The dotted red line depicts an additive phenotype; note the synthetically enhanced (i.e. larger than additive) number of incomplete walls. Mean ± S.E.M. ***p = 3 e^{-06} for a comparison between *trs120-4* and double mutants; Student's two-tailed t test. n = 20 wild type (Col-0), n = 3 *ple-2*, n = 18 *trs120-4* and n = 9 *ple-2 trs120-4* seedlings.

Figure 3. Colocalization between TRS120-mCherry and GFP-PLEIADE in meristematic arabidopsis root cells.
(a) Time lapse of P_{PLE}::GFP-PLEIADE with the P_{UBQ}::TRS120-mCherry TRAPPII subunit is shown, with minutes indicated in the right panel. The markers co-localize throughout cytokinesis. Arrowheads point to leading edges of the cell plate. Bars = 10 µm.
(b) The line graphs depict scaled relative intensity of GFP-PLEIADE and TRS120-mCherry at the cell plate. Note that throughout cytokinesis almost every peak of GFP-PLEIADE fluorescence coincides with a peak of TRS120-mCherry fluorescence (black arrowheads).

Figure 4. Localization of TRAPPII and PLEIADE/AtMAP65-3 gene fusions in mutant backgrounds.
(a-c) Time lapses are shown, with minutes indicated in the right panel. Arrowheads point to leading edges of the cell plate. Bars = 10 µm.
(a) P_{PLE}::GFP-PLEIADE time lapse in *club-2*, a TRAPPII null mutant. Note the punctate appearance of the cell plate. Also, within a 28 minute time lapse, GFP-PLEIADE has failed to reorganize to the leading edges of the cell plate, suggestive of an impairment in MT dynamics.

(b) Antibody stains in P_{PLE}::GFP-PLEIADE root tips. DAPI/nucleus (white); microtubules (red) anti-GFP; and merge. Note that in *club-2* mutants (lower panel), GFP-PLEIADE is found at the midzone of patchy phragmoplasts (open arrowhead). Bars = 10 µm.
(c) TRS120-GFP in *ple-4*, a null allele of the AtMAP65-3 locus. Note the diffuse appearance of both TRS120-GFP and FM4-64.
(d) Thickness of cell plate in µm, as assessed with TRS120-GFP (green) or FM4-64 (red) in wild type and *ple-4* root tips. Mean ± S.E.M. Wild type n = 6 cell plates and 24 measurements; *ple-4* n = 18 cell plates and 70 measurements.

Figure 5. Characterization of TRAPPII and pleiade single and double mutants. See also Figure S3.
(a) Antibody stains of root tips. DAPI/nucleus (white); microtubules (red); and merge. Bars = 10 µm. Note the absence of multinucleate cells in wild type and *trs120-4*, but the binucleate cell in *ple-2* (asterisk) and the multinucleate cells in the *ple-2 trs120-4* double mutant.
(b) A multinucleate cell characteristic of the double mutant, in which seven nuclei are clumped together in the absence of even vestigial cross walls.
(c) % multinucleate cells lacking cross walls or stubs. Mean ± S.E.M. The horizontal dotted red line depicts an additive phenotype. *p = 0,03 for a comparison between *ple-2* and *ple-2 trs120-4* for 2-3 nuclei; ***p = 3 e^{-05} for a comparison between *ple-2* and *ple-2 trs120-4* for 4 or more nuclei; Student's two-tailed t test; wild type: n = 1798 cells; *trs120-4*: n = 1123 cells; *ple-2*: n = 4136 cells; *ple-2 trs120-4*: n = 1185 cells.
(d) Toluidine-blue stained histological sections of mutant embryos. Bars = 10 µm.
Wild-type embryo (left panel).
ple-4 embryo (middle and right panels); note that the cytokinesis defect is more pronounced in the radicle, which may explain why we did not detect co-purified MAP65-3 from inflorescences.
(e) Focused Ion Beam/Scanning Electron Micrographs of high pressure frozen, freeze substituted five-day old root tips. Single slices are shown in the left panel and 3D reconstructions of entire stacks in the right panel. Nuclei (N): blue spherical structures; cross walls: green; cell outline: beige. Bars = 10 µm. Wild type (upper panel); note the regular shape of the cell and the complete cross wall. *ple- 4* (lower panel); note that there are two nuclei but no apparent cross wall in the 3D reconstruction (lower right panel).
(f) A conceptual framework for the integration of cell cycle cues with membrane and microtubule dynamics during plant cytokinesis. MAP65 proteins are targets of cell cycle regulated kinases (Kosetsu et al., 2010; Sasabe et al. 2011a, 2011b) and PLEIADE/AtMAP65-3 also interacts with spindle assembly checkpoint (SAC) proteins (Paganelli et al., 2015). The TRAPPII-MAP65 interaction would thereby transmit cues

pertaining to cell cycle progression and chromosome attachment to the trafficking apparatus at the cell plate, while ensuring the coordination of membrane and microtubule dynamics throughout cytokinesis. The depicted interactions are published (black) or documented by multiple lines of evidence in this contribution (green). The thickness of the line is proportional to the number of lines of evidence that document the interaction.

Table I. Analysis of CLUB-GFP immunoprecipitates (IPs) via mass spectrometry. This table lists only microtubule-related proteins with a possible role in plus-end tracking or a microtubule stabilizing role detected in the IPs. The data are based on three biological replicates.

molecular function	AGI[a]	LOCUS NAME	p value in proteomic screen[b]	coexpression coefficient[c]	biological role (cellular phenotype)[d]	References
Stabilizing MAP	At5g55230	AtMAP65-1	0,008	0.53	binds and bundles MTs, stabilizes MTs, promotes nucleation. Is involved in mitotic cell cycle.	(Smertenko et al., 2004; Van Damme et al., 2004; Mao et al., 2005; Sasabe et al., 2011b)
+TIP	At4g27060	TOR1/SPR2	0,00003	0.48	plant-specific MAP that regulates the orientation of cortical MTs and organ growth. Is involved in mitotic cell cycle	(Yao et al., 2008; Wightman et al., 2013)
	At2g20190	AtCLASP	0,002	0.57	MAP215 member involved in cell division and cell expansion. Is thought to promote MT stability.	(Ambrose et al., 2007, 2011; Ambrose and Wasteneys, 2008; Kirik et al., 2007; Pietra et al., 2013)
	At2g35630	MOR1	0,00006	0.44	MAP215 member required for cortical MT organization. Required for cell division, cell expansion and root hair polarity.	(Eleftheriou et al., 2005; Kawamura et al., 2006; Lechner et al., 2012; Twell et al., 2002; Whittington et al., 2001)

a: (AGI) Arabidopsis genome initiative accessions (www.arabidopsis.org).

b: p values (< 0.002) were calculated using the t-test (two-sided). See Table S1 for the quality and specificity of the hits, which is comparable to that of known TRAPP interactors of CLUB/AtTRS130 (Table S1; Rybak et al., 2014).

c: Coexpression coefficients (Genevestigator (Hruz et al., 2008), perturbations), were similar to those found for other TRAPP components (see Table S1).

d: as seen by gene ontology annotation on www.arabidopsis.org (Swarbreck et al., 2007).

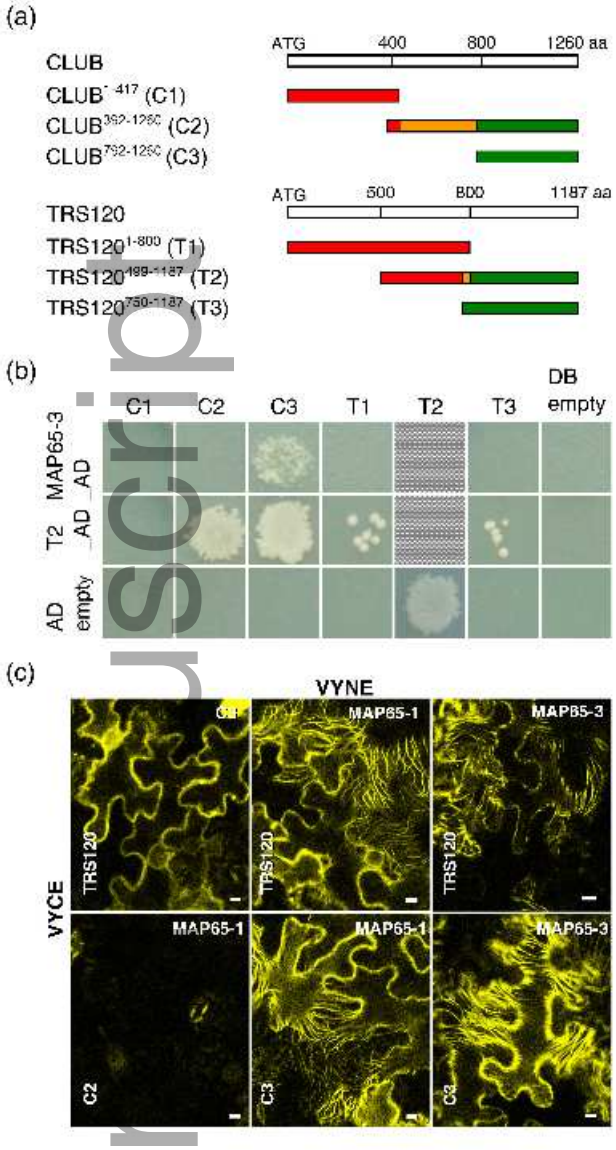

Figure 1. Physical interaction between the TRAPPII complex and MAP65 proteins. See also Figure S1.
(a) TRAPPII truncations used for binary interaction assays. Segments colored in red are conserved across kingdoms, while ones in green are plant-specific. The orange moiety of the C2 segment is poorly conserved across kingdoms. The T2 middle segment corresponds to sequences found to interact with the exocyst in a yeast two-hybrid screen (Rybak et al., 2014).
(b) Yeast two-hybrid experiments, the panels are spliced together from different plates. Note positive interactions between the plant specific C3_DB CLUB/AtTRS130 truncation and AtMAP65-3_AD, and between CLUB C2_DB or C3_DB and T2_AD. T2_DB is an auto activator, as evidenced by colony growth with the empty AD vector, and this precludes our ability to determine whether AtTRS120_T2 interacts with PLEIADE/AtMAP65-3.
(c) BiFC experiments. VYNE and VYCE vectors represent fusions of the specified proteins or protein fragments to N- and C-terminal YFP moieties. The CLUB-C3 truncation and AtTRS120 full-length protein interact with AtMAP65-1 and AtMAP65-3. This interaction is localized to an ordered, linear array reminiscent of cortical microtubules. By contrast, TRAPPII complex interactions (here CLUB_C3 is shown to interact with TRS120) are localized to intracellular membranes and to the cytosol. As a negative control, AtMAP65-1 does not interact with the CLUB_C2 truncation. Bars = 10 µm.

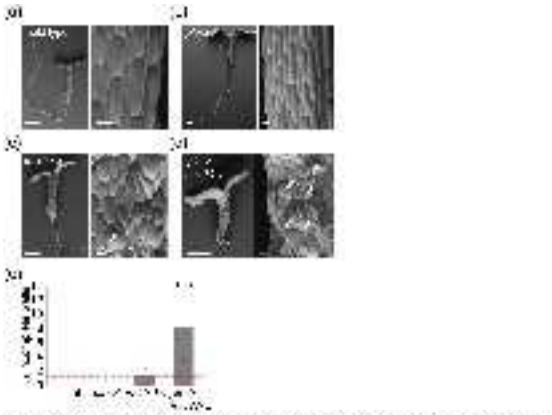

Figure 2. Genetic interaction between the TIC/TOC complex and VARS proteins

tpj_13275_f2.jpg

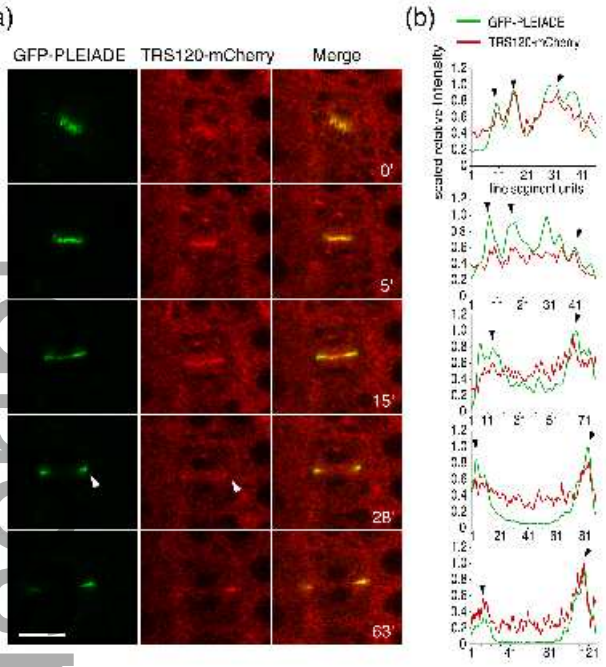

Figure 3. Colocalization between TRS120-mCherry and GFP-PLEIADE in meristematic arabidopsis root cells.

(a) Time lapse of P_{PLE}::GFP-PLEIADE with the P_{UBQ}::TRS120-mCherry TRAPPII subunit is shown, with minutes indicated in the right panel. The markers co-localize throughout cytokinesis. Arrowheads point to leading edges of the cell plate. Bars = 10 μm.

(b) The line graphs depict scaled relative intensity of GFP-PLEIADE and TRS120-mCherry at the cell plate. Note that throughout cytokinesis almost every peak of GFP-PLEIADE fluorescence coincides with a peak of TRS120-mCherry fluorescence (black arrowheads).

tpj_13275_f3.jpg

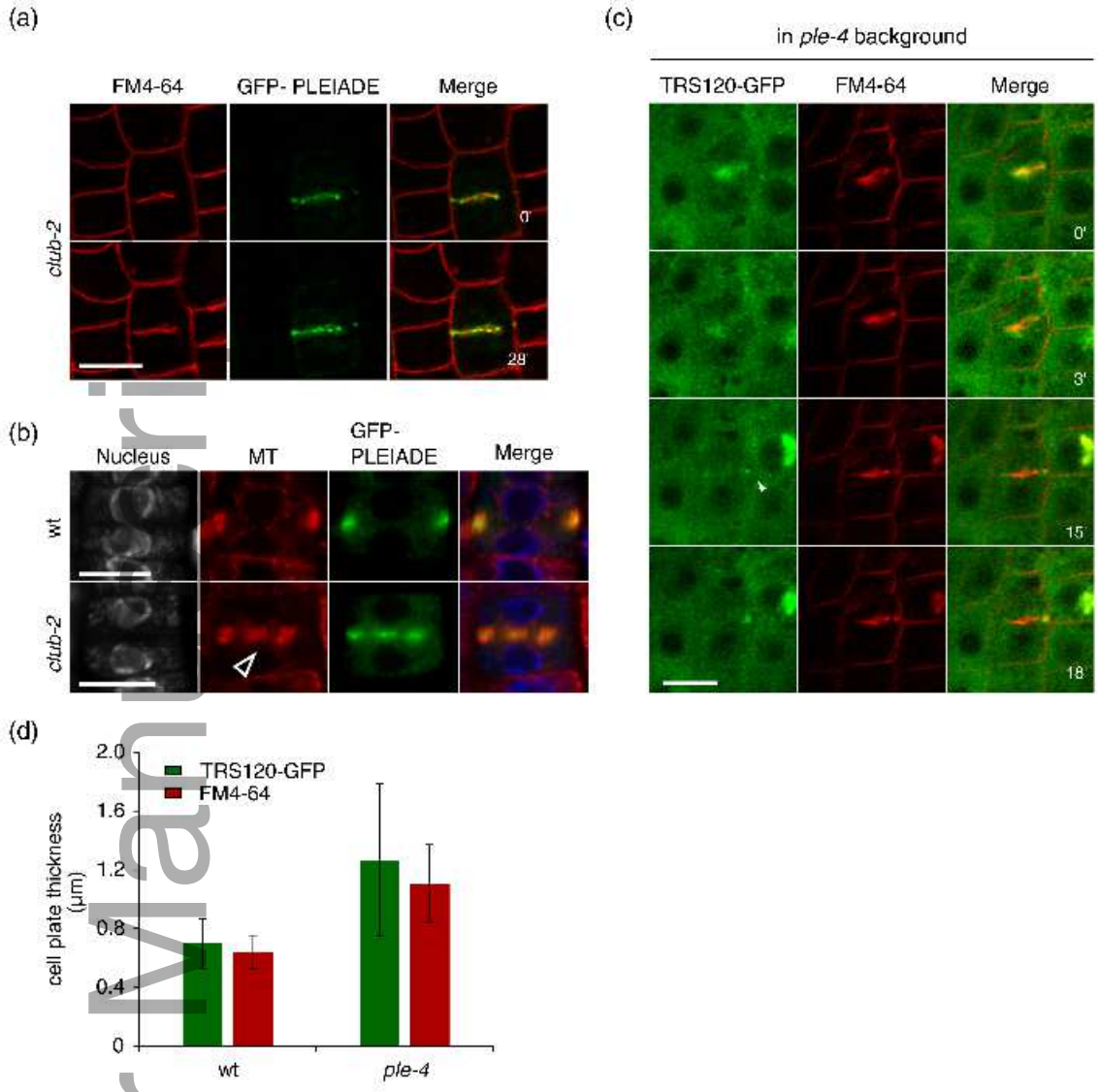

Figure 4. Localization of TRAPPII and PLEIADE/AtMAP65-3 gene fusions in mutant backgrounds.
(a-c) Time lapses are shown, with minutes indicated in the right panel. Arrowheads point to leading edges of the cell plate. Bars = 10 µm.
(a) P_{PLE}::GFP-PLEIADE time lapse in *club-2*, a *TRAPPII* null mutant. Note the punctate appearance of the cell plate. Also, within a 28 minute time lapse, GFP-PLEIADE has failed to reorganize to the leading edges of the cell plate, suggestive of an impairment in MT dynamics.
(b) Antibody stains in P_{PLE}::GFP-PLEIADE root tips. DAPI/nucleus (white); microtubules (red) anti-GFP; and merge. Note that in *club-2* mutants (lower panel), GFP-PLEIADE is found at the midzone of patchy phragmoplasts (open arrowhead). Bars = 10 µm.
(c) TRS120-GFP in *ple-4*, a null allele of the *AtMAP65-3* locus. Note the diffuse appearance of both TRS120-GFP and FM4-64.
(d) Thickness of cell plate in µm, as assessed with TRS120-GFP (green) or FM4-64 (red) in wild type and *ple-4* root tips. Mean ± S.E.M. Wild type n = 6 cell plates and 24 measurements; *ple-4* n = 18 cell plates and 70 measurements.

tpj_13275_f4.jpg

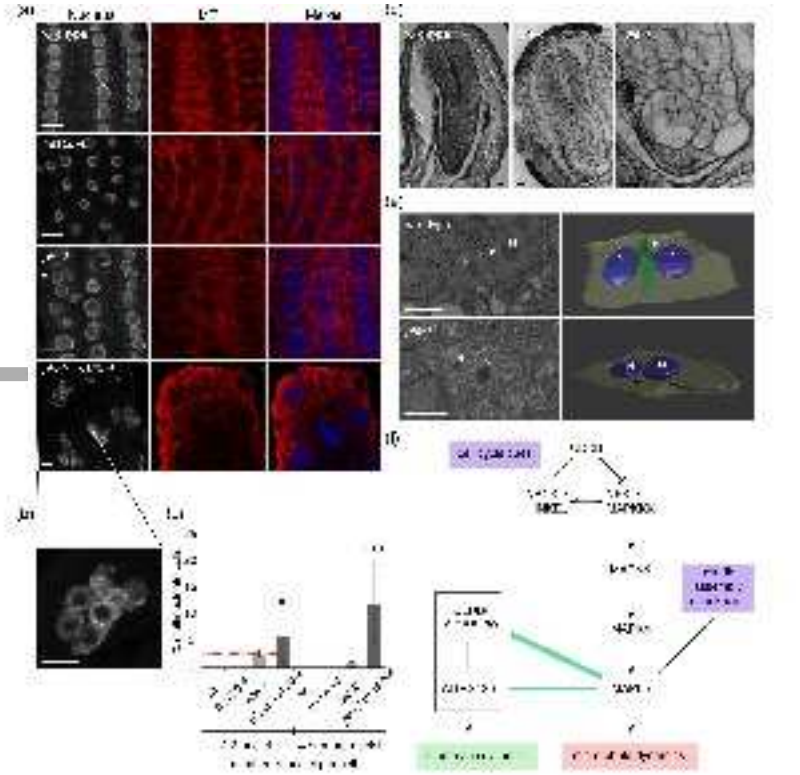

tpj_13275_f5.jpg